Structure of a Substrate Radical Intermediate in the Reaction of Lysine 2,3-Aminomutase†

Marcus D. Ballinger, Perry A. Frey,* and George H. Reed*

The Institute for Enzyme Research, Graduate School, and Department of Biochemistry, College of Agricultural and Life Sciences, University of Wisconsin, Madison, Wisconsin 53705

Received June 16, 1992; Revised Manuscript Received August 28, 1992

ABSTRACT: Electron paramagnetic resonance (EPR) spectroscopy has been used to characterize an organic radical that appears in the steady state of the reaction catalyzed by lysine 2,3-aminomutase from *Clostridium* SB4. Results of a previous electron paramagnetic resonance (EPR) study [Ballinger, M. D., Reed, G. H., & Frey, P. A. (1992) *Biochemistry 31*, 949–953] demonstrated the presence of EPR signals from an organic radical in reaction mixtures of the enzyme. The materialization of these signals depended upon the presence of the enzyme, all of its cofactors, and the substrate, lysine. Changes in the EPR spectrum in response to deuteration in the substrate implicated the carbon skeleton of lysine as host for the radical center. This radical has been further characterized by EPR measurements on samples with isotopically substituted forms of lysine and by analysis of the hyperfine splittings in resolution-enhanced spectra by computer simulations. Changes in the hyperfine splitting patterns in EPR spectra from samples with [2-^{2}H]lysine and [2-^{13}C]-lysine show that the paramagnetic species is a π-radical with the unpaired spin localized primarily in a p orbital on C2 of β-lysine. In the EPR spectrum of this radical, the α-proton, the β-nitrogen, and the β-proton are responsible for the hyperfine structure. Analysis of spectra for reactions initiated with L-lysine, [3,3,4,4,5,5,6,6-^{2}H$_8$]lysine, [2-^{2}H]lysine, perdeuteriolysine, [α-^{15}N]lysine, and [α-^{15}N,2-^{2}H]lysine permit a self-consistent assignment of hyperfine splittings. The large, virtually isotropic hyperfine splitting from nitrogen on the β-carbon combined with a small hyperfine splitting from the β-proton shows that the dihedral angles between the axis of the singly occupied p orbital on C_α and the C_β–H, and C_β–N bonds are approximately 70°, and 10°, respectively. These spectroscopic observations provide strong support for a rearrangement involving radicals derived from the substrate as intermediates.

Organic radical intermediates that derive from substrates, coenzymes, or amino acid residues have been implicated in a growing number of enzymatic reactions (Edmondson, 1978; Stubbe, 1989; Frey, 1990). Enzyme-catalyzed 1,2 rearrangements which are dependent upon the coenzyme, adenosylcobalamin (B_{12}), are among the most extensively researched. In these reactions, a radical fragment of adenosylcobalamin, 5′-deoxyadenosine-5′-yl, is believed to initiate the rearrangements through the abstraction of a hydrogen atom from an unactivated carbon of the substrate to give a substrate radical intermediate and 5′-deoxyadenosine. The radical intermediate undergoes a rearrangement and regains a hydrogen atom from 5′-deoxyadenosine to regenerate the radical cofactor and form the product (Abeles & Dolphin, 1976). EPR[1] spectroscopic evidence for radical intermediates has been presented for the B_{12}-dependent reactions of ethanolamine ammonia-lyase (Babior et al., 1974; O'Brien, et al., 1985; Tan et al., 1986), ribonucleotide reductase (Hamilton et al., 1972), and diol dehydrases (Cockle et al., 1972; Finlay et al., 1973; Valinsky et al., 1974).

Lysine 2,3-aminomutase from *Clostridia* catalyzes a 1,2 rearrangement in the conversion of L-lysine to L-β-lysine. This hexameric protein (MW 285 000) does not contain vitamin B_{12} (Petrovich et al., 1991). Rather, the enzyme contains iron sulfur centers, Co, and PLP (Petrovich et al., 1991). *S*-Adenosylmethionine is required to activate the enzyme (Chirpich et al., 1970), and this activation is thought to take place by reaction with a reduced metal center, leading to the formation of a reactive adenosyl-metal cofactor (Petrovich et al., 1991; Moss & Frey, 1990). This species would then undergo reversible homolytic cleavage, generating 5′-deoxyadenosine-5′-yl.

A hypothetical rearrangement mechanism initiated by 5′-deoxyadenosine-5′-yl is outlined in Scheme I. In this mechanism, the 5′-deoxyadenosine-5′-yl abstracts a hydrogen from carbon 3 of the imine formed between lysine and PLP. The 1,2-imino shift ensues, facilitated by the PLP via an azacyclopropylcarbinyl radical intermediate. Chemical evidence for this mechanism is provided by the demonstration of hydrogen transfer among the 5′-position of *S*-adenosylmethionine, lysine, and β-lysine (Moss & Frey, 1987; Baraniak et al., 1989, Kilgore & Aberhart, 1991), and cleavage of *S*-adenosylmethionine to 5′-deoxyadenosine and methionine (Moss & Frey, 1990). The mechanism is also supported by the discovery of a chemical precedent for the rearrangement (Han & Frey, 1990).

In addition to 5′-deoxyadenosine-5′-yl, Scheme I includes three distinct radical intermediates-in two of which unpaired spin density resides on the carbon skeleton of the substrate or product. A previous paper reported EPR signals from one or more organic radicals that were observed in reaction mixtures of lysine 2,3-aminomutase that had been frozen in the steady state of the reaction (Ballinger et al., 1992). These EPR signals were observed only in the presence of L-lysine and

† This work was supported by Grants DK28607 (P.A.F.) and GM35752 (G.H.R.) from the NIH and by an NRSA Fellowship (M.D.B.) from NIH Training Grant GM08293.

[1] Abbreviations: EPR, electron paramagnetic resonance; NMR, nuclear magnetic resonance; PLP, pyridoxal 5′-phosphate; S/N, signal to noise ratio; CW, continuous wave, B_{12r}, vitamin B_{12} with Co in the +2 oxidation state; *a*, the isotropic hyperfine splitting constant; A_{ii} ($i = x, y, z$), the principal component of the hyperfine splitting tensor along the *i*th axis.

0006-2960/92/0431-10782$03.00/0

Scheme I

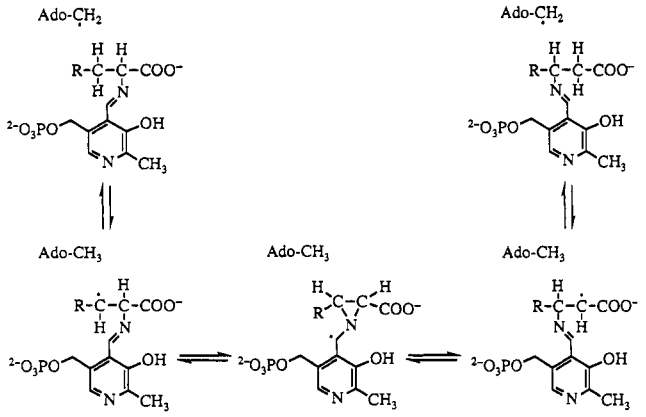

S-adenosylmethionine in the reaction mixture, and their intensity correlated linearly with enzyme activity. Furthermore, a prominent improvement in the resolution of hyperfine features in EPR spectra of a sample initiated with L-[3,3,4,4,5,5,6,6-$^2H_8$]lysine suggested that there was appreciable spin density on the carbon skeleton of lysine. These results prompted a more detailed study of the EPR properties of the intermediate(s) by isotropic substitutions in the substrate, lysine. The present paper reports the structural characterization of the steady-state radical intermediate in the lysine 2,3-aminomutase reaction by EPR spectroscopy.

EXPERIMENTAL PROCEDURES

Enzyme Purification and Assay. Lysine 2,3-aminomutase was purified by procedures described previously (Petrovich et al., 1991; Moss & Frey, 1990). Activities of samples under conditions used in EPR measurements were monitored by radiochemical assay as detailed earlier (Ballinger et al., 1992).

Labeled Lysines. L-[3,3,4,4,5,5,6,6-$^2H_8$]-, L-[4,4,5,5-$^2H_4$]-, and L-[2-^{13}C]lysine were obtained from MSD isotopes, and L-[α-^{15}N]lysine was from Cambridge Isotopes. DL-[2-^{2}H]-lysine hydrochloride was synthesized using the method of Battersby et al. (1982), using the following modifications. The α-deuterium exchange procedure was performed on N^{α},N^{ϵ}-diacetyllysine using a 20-fold molar excess of acetic anhydride and 99.9% ^2H_2O. Solvent was removed, and the exchange was repeated with fresh solvent. Integrals of the NMR signals at δ = 3.73 ppm (^2H_2O solvent) corresponding to the residual 2-^{1}H of lysine showed >92% ^{2}H incorporation specifically at that position. This procedure was also used for the synthesis of DL-[α-^{15}N,2-^{2}H]- and DL-[$^2H_9$]lysine from the corresponding labeled lysines mentioned above. The L-enantiomers of the DL-lysine mixtures were not resolved, because D-lysine did not inhibit lysine 2,3-aminomutase or adversely affect EPR spectra.

EPR Measurements. Preparation of samples was carried out as described in the previous paper (Ballinger et al., 1992). Samples were frozen during the steady state of the reaction (i.e., 30 s–1 min after initiation of the reaction) and kept in liquid N_2. EPR spectra were recorded at X-band on a Varian E-3 spectrometer. The microwave frequency was calibrated with a Hewlett Packard X532B frequency meter, and the magnetic field was calibrated with a Varian gaussmeter. A liquid N_2 immersion dewar (Suprasil Quartz, Wilmad Glass Co.) was used to maintain samples at 77 K. The spectrometer was interfaced with a PC AT microcomputer for data acquisition. Scan averaging was employed to improve S/N for subsequent resolution enhancement. EPR data were uploaded to a VAX 3100 M76 workstation for resolution enhancement.

EPR Data Treatment and Simulations. To aid in identification of hyperfine features in the experimentally observed EPR spectra, the spectra were resolution enhanced by methods analogous to those described previously (Hedberg & Ehrenberg, 1968; Kauppinen et al., 1981; Latwesen et al., 1992). The spectra were Fourier transformed, deconvoluted with a Lorentzian function, $\exp(2\pi\sigma|t|)$ (where σ is the line width), apodized with a squared Bartlett window function, $(1 - |x|/L)^2$, and inverse transformed to the frequency domain (Latwesen et al., 1992). The parameters used in resolution enhancement, σ and L, were chosen according to the guidelines given by Kauppinen et al. (1981).

Spectral simulations were computed by numerical integration of the following expression (Hecht, 1967):

$$\frac{dF}{dH} = \int_0^{2\pi}\int_0^{\pi}\frac{dG}{dH}\sin\theta\, d\theta\, d\phi \qquad (1)$$

where G is a Gaussian lineshape function centered at a field position, H_r, and θ and ϕ are, respectively, the polar and azimuthal angles of the magnetic field vector in the principal coordinate system. H_r was calculated using the following first-order expression (Hecht, 1967):[2]

$$H_r = \frac{h\nu}{g(\theta,\phi)\,\beta} - \sum_k \frac{K_k(\theta,\phi)}{g(\theta,\phi)\,\beta}M_k \qquad (2)$$

In eq 2, $g(\theta,\phi) = (g_{xx}^2\sin^2\theta\cos^2\phi + g_{yy}^2\sin^2\theta\sin^2\phi + g_{zz}^2\cos^2\theta)^{1/2}$, $K_k(\theta,\phi) = (1/g(\theta,\phi))(A_{xx}^2g_{xx}^2\sin^2\theta\cos^2\phi + A_{yy}^2 g_{yy}^2\sin^2\theta\sin^2\phi + A_{zz}^2g_{zz}^2\cos^2\theta)^{1/2}$, and each nucleus contributes $2I + 1$ hyperfine lines. A Gaussian lineshape provided a reasonable approximation to the lineshape of the resolution-enhanced signals. This level of analysis neglects effects from the smaller nuclear Zeeman and nuclear quadrupolar terms. For simulations that included the hyperfine interaction of the β-proton, the nuclear hyperfine term in eq 2 was modified to include the trigonometric functions of the Euler angles (α,β,γ) relating the principal axes of the β-proton hyperfine tensor to the principal axes of the **g** tensor (Rieger, 1982).

Computer programs were written in FORTRAN and run on the VAX workstation. Between 900 and 2000 crystallite orientations were sampled in the simulations which typically required <30 s for execution. Fitting was done by visual comparison of experimental and computed spectra.

RESULTS

Location of the Radical Center. Results of the previous study indicated that the EPR signals obtained from samples that were frozen in the steady state contained fewer components than those from samples frozen after the reaction had reached equilibrium. Identification of the sources of hyperfine splitting in this predominant, steady-state radical spectrum was therefore pursued. Previous EPR measurements on samples made up with L-[3,3,4,4,5,5,6,6-$^2H_8$]lysine (L-[$^2H_8$]lysine)

[2] Some simulations were repeated using the second-order expressions of Atherton and Winscom (1973) for H_r. These simulations were virtually identical to those computed with the above expressions and confirmed that the second-order corrections are negligible in the present applications. The adequacy of first-order expressions for simulation of free-radical EPR spectra at X-band has also been verified by Brok et al. (1986).

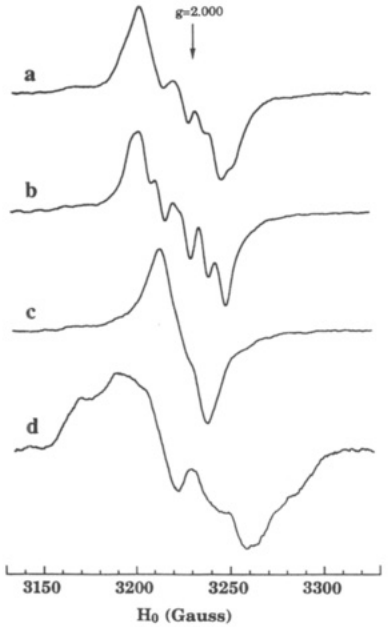

FIGURE 1: EPR spectra (77 K) of steady-state reaction mixtures with isotopically substituted lysines. Samples contained lysine 2,3-aminomutase (30–35 μM oligomer concentration) after 4 h of reductive activation [see Ballinger et al. (1992)], Tris-HCl at pH 8.0 (50 mM), sodium dithionite (30 mM), *S*-adenosylmethionine (1.2 mM), and the following forms of lysine (200 mM): (a) L-lysine (unlabeled), (b) L-[3,3,4,4,5,5,6,6-$^2H_8$]lysine, (c) DL-[2-^{2}H]lysine, and (d) L-[2-^{13}C]lysine. All spectra were accumulated from 20 scans (4 min/scan); the microwave frequency was 9.044 GHz.

showed that protons from C3 to C6 of lysine are weakly coupled to the unpaired electron spin (Ballinger et al., 1992). The spectrum of the sample with [$^2H_8$]lysine retains a similar overall splitting pattern as the unlabeled compound, but individual features are narrowed (Figure 1, spectra a and b).

The position of the radical center is apparent from EPR spectra of samples prepared either with [2-^{2}H]lysine or with [2-^{13}C]lysine (Figure 1, spectra c and d). The hyperfine splitting pattern collapses upon substitution of ^{2}H for ^{1}H at C2 of lysine. Furthermore, introduction of ^{13}C at C2 of lysine results in a new, large, splitting of a magnitude comparable with the central atom hyperfine splittings measured for several π-radicals (Morton, 1964). Spectra of these two samples demonstrate that the paramagnetic species is a π-radical with the unpaired electron in a p orbital on C2 of the lysine skeleton.

Sources of Hyperfine Splitting. In addition to the α-proton, the unpaired electron could be coupled to the β-proton, the nitrogen of the migratory amino group, and possibly protons more remote from the radical center. Protons on carbons 4 and 5, however, are not a significant source of splitting, as evidenced by the absence of changes in the EPR spectrum when [4,4,5,5-$^2H_4$]lysine is used as a substrate (spectrum not shown). This observation indicates that changes in the hyperfine pattern in spectra of samples with [$^2H_8$]lysine in place of lysine (Figure 1, spectrum b) are solely due to deuterium substitution at the β-carbon. Participation of the migratory nitrogen in the hyperfine splitting becomes evident upon substitution of ^{15}N for ^{14}N in the α-amino group of the substrate. With either [α-^{15}N]lysine or [α-^{15}N,2-^{2}H]lysine as substrate, the resulting EPR spectra exhibit changes in the splitting patterns relative to those in spectra of samples with their respective ^{14}N counterparts (Figure 2). Given the location of the radical center at C2 and the presence of the α-proton, the spin-coupled nitrogen must be attached to the β-carbon. Finally, the lack of appreciable changes in the

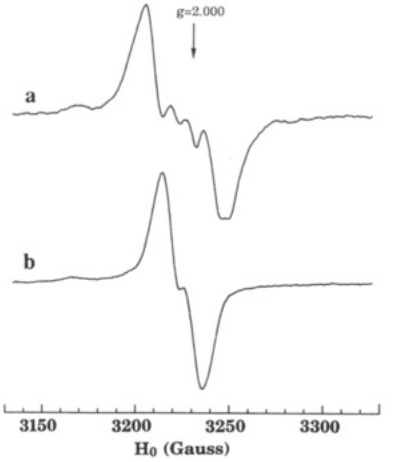

FIGURE 2: EPR spectra (77 K) of steady-state reaction mixtures with [^{15}N]lysines: (a) L-[α-^{15}N]lysine and (b) DL-[α-^{15}N, 2-^{2}H]lysine. Other conditions are given in the legend for Figure 1.

Scheme II

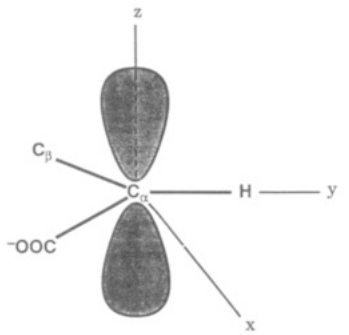

spectrum obtained from a reaction carried out in 77% ^2H_2O indicates that solvent-exchangeable protons are not strongly coupled to the radical (Ballinger et al., 1992). All of these experimental observations indicate that the paramagnetic species is an α-radical of a form of β-lysine (see Scheme I). Furthermore, the hyperfine structure in the EPR spectrum of this radical arises from hyperfine coupling between the unpaired electron and the α-proton, the β-proton, and the β-nitrogen.

Analysis of EPR Spectra. α-Carbon-based radicals of carboxylic acids have been studied extensively, e.g., in single crystals exposed to ionizing radiation (McConnell et al., 1960; Morton, 1964; Fisher, 1973). These radicals belong to a larger class of π-alkyl radicals that are among the best characterized of all organic free radicals (Wertz & Bolton, 1986). The powder spectra obtained in the present experiments are more challenging to analyze than spectra of single crystals because the principal values of the relevant tensors must be extracted from "turning points" in the absorption envelopes rather than from the orientation dependencies of resolved splittings. Resolution enhancement of the powder spectra, combined with computer simulations and isotropic substitutions, however, provides a means to determine the respective hyperfine splitting constants from the CW EPR spectra.

A characteristic, and dominant, EPR spectral feature of π-alkyl radicals is the hyperfine splitting tensor from the α-proton(s) (Wertz & Bolton, 1986). Hyperfine splittings from nuclear spins attached to the β-carbon are typically nearly isotropic due to their increased distance from the center of unpaired spin and to their predominantly hyperconjugative origin (Morton, 1964). The structure of the lysine radical including the principal axes is shown in Scheme II.

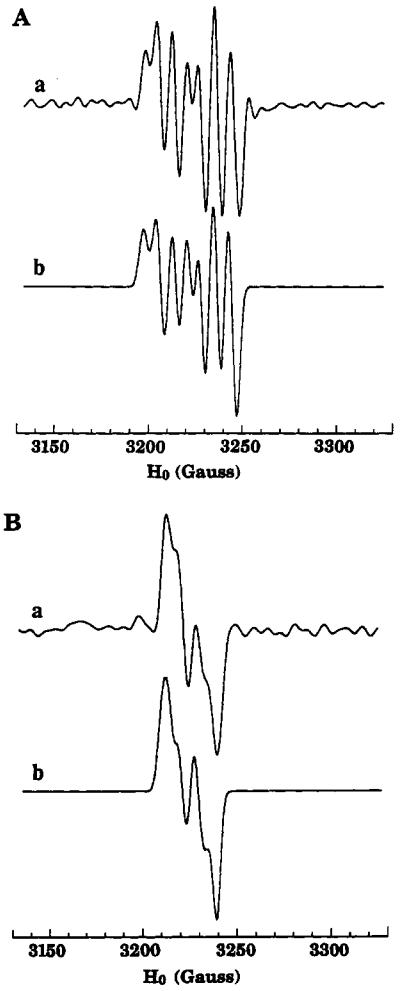

FIGURE 3: Comparison of resolution enhanced experimental (a) and computer simulated (b) spectra of samples prepared with L-[3,3,4,4,5,5,6,6-$^2H_8$]lysine (A) and DL-[$^2H_9$]lysine (B). The spectrum recorded experimentally for spectrum a in part A is shown in spectrum b of Figure 1. Resolution enhanced spectra were obtained using (A, a) σ = 7.5 G and L = 0.195 G^{-1} and (B, a) σ = 6.5 G and L = 0.180 G^{-1}. Simulations were obtained using g_{xx} = 2.0043, g_{yy} = 2.0037, g_{zz} = 2.0021, $a^{14}_{N\beta}$ = 8.3 G; for α-^{1}H (A, b), A_{xx} = 32.6 G, A_{yy} = 10.1 G, A_{zz} = 22.5 G; and for α-^{2}H (B, b), A_{xx} = 5.0 G, A_{yy} = 1.6 G, A_{zz} = 3.5 G. Line widths were (A, b) 2.5 G and (B, b) 2.6 G; 2025 crystal orientations were sampled in the simulations.

The **g** tensor and α-proton hyperfine splitting tensor typical of α-carbon radicals of carboxylic acids provided a logical framework for initial attempts at simulating the spectra of the α-radical of β-lysine. Individual parameters were then varied until reasonable coincidence was achieved in the positions of features in the experimentally observed and computed spectra. These parameters, or derivatives thereof appropriate for an isotopic substitution, were then applied in an iterative manner to simulation of spectra from samples with various isotopically substituted lysines. The ranges of hyperfine splitting parameters were stringently constrained by the requirement for a simultaneous fit to the hyperfine structure in all of the spectra from samples with isotopic substitutions for each of the three coupled nuclei. This iterative procedure ultimately yielded a single, self-consistent set of **g** values and hyperfine splitting parameters.

α-Proton Hyperfine Tensor and Nitrogen Hyperfine Splittings. Splitting from the α-proton is most readily analyzed in the spectrum of the sample prepared with [$^2H_8$]lysine. Figure 3A shows a comparison of experimental (a) and computed (b) spectra of this sample. The principal values of the α-proton tensor used in the simulation (see Table I) and the **g** tensor

Table I: Hyperfine Splitting Parameters Obtained from Spectral Simulations[a]

		principal values of hyperfine tensor[b] (G)		
nucleus	a_0 (G)	A_{xx}	A_{yy}	A_{zz}
$^1H_\alpha$	−21.7 ± 0.5	−32.6 ± 0.8	−10.1 ± 0.8	−22.5 ± 0.8
$^2H_\alpha$[c]	−3.4 ± 0.1	−5.0 ± 0.1	−1.6 ± 0.1	−3.5 ± 0.1
$^1H_\beta$[d]	+5.3 ± 0.5	+3.6 ± 0.8	+3.6 ± 0.8	+8.8 ± 0.8
$^{14}N_\beta$	(±)8.3 ± 0.5		isotropic	
$^{15}N_\beta$[e]	(∓)11.6 ± 0.7		isotropic	
$^{13}C_\alpha$	+31 ± 3	+8.6 ± 5	+8.6 ± 5	+76 ± 5

[a] The principal values of the g tensor are: g_{xx} = 2.0043; g_{yy} = 2.0037; g_{zz} = 2.0021. [b] The empirical nature of the fitting procedure precludes a rigorous error analysis. The uncertainties given are estimates based on an ability to visualize deviations in the computed spectra. The signs of the hyperfine splittings are assigned based on literature precedents (Wertz & Bolton, 1986). [c] These values were calculated from the respective values for the α-proton. [d] The principal axes for this tensor are related to the principal axes of the g tensor by Euler angles: α = 3°; β = −80°; γ = 0°. [e] Calculated from the value for ^{14}N. The sign of this splitting constant will be opposite to that of ^{14}N because of the negative magnetogyric ratio of ^{15}N.

(g_{xx} = 2.0043; g_{yy} = 2.0037; g_{zz} = 2.0021) are similar to those reported for other radicals of α-carboxylic acids (Morton, 1964). The well-resolved splittings on the high-field half of the spectrum constitute the "signature" of this radical, and these splittings are due to a large (a^{14}_N = 8.3 G), isotropic ^{14}N hyperfine splitting.

Simulation of spectra for samples with substitution of ^{2}H at C2 requires inclusion of the hyperfine structure from the α-deuteron. The principal values of the α-deuteron tensor are calculated from those of the α-proton by multiplication of the latter by $\gamma_{^2H}/\gamma_{^1H}$. This tensor, together with the triplet multiplicity for ^{2}H and the other parameters used in Figure 3A, provides satisfactory simulation of the spectrum obtained for the sample with [$^2H_9$]lysine (Figure 3B).

The magnitude of the ^{14}N hyperfine splitting was verified by simulation of spectra obtained with [α-^{15}N]-substituted lysines. The splitting constant, $a_{^{15}N}$, is calculated from that of ^{14}N ($a_{^{15}N} = a_{^{14}N}(\gamma_{^{15}N}/\gamma_{^{14}N})$), and this doublet splitting, together with the hyperfine splitting of the β-proton, α-proton (α-deuteron), models the spectra obtained from samples with [α-^{15}N]- and [α-^{15}N,2-^{2}H]lysine (Figure 4). ^{14}N hyperfine splittings of this magnitude have been observed in several other π-radicals containing β-amino groups (Paul & Fisher, 1969; Taniguchi et al., 1968; Armstrong & Humphreys, 1967).

Hyperfine Splitting from the β-Proton. The magnitude of hyperfine splitting from β-protons in π-radicals can be comparable to that of the α-protons (Wertz & Bolton, 1986). The data of Figure 1, however, indicate that the hyperfine coupling from the β-proton in this radical is relatively weak. In characterizing the β-proton hyperfine interaction, the isotropic component, $a_{\beta H}$, was first estimated by incorporating an isotropic doublet splitting into simulations of spectra obtained from samples with either [2-^{2}H]lysine or unlabeled lysine. The widths of the splitting manifolds were best simulated with $a_{\beta H}$ between 5 and 6 G. An isotropic splitting, however, did not adequately reproduce the shapes of the splitting patterns observed in spectra containing hyperfine interactions from the β-proton, and this effect was traced to anisotropy in the β-proton hyperfine splitting.

An upper limit on the magnitude of the anisotropic (dipole–dipole) splitting from the β-proton can be calculated from the C2–H_β distance (2.14 Å) and the classical point–dipole approximation (Goodman & Raynor, 1970). The z' principal axis of this dipolar interaction is along a line from C2 to H_β, and the orientation of the z' axis in the principal axis system

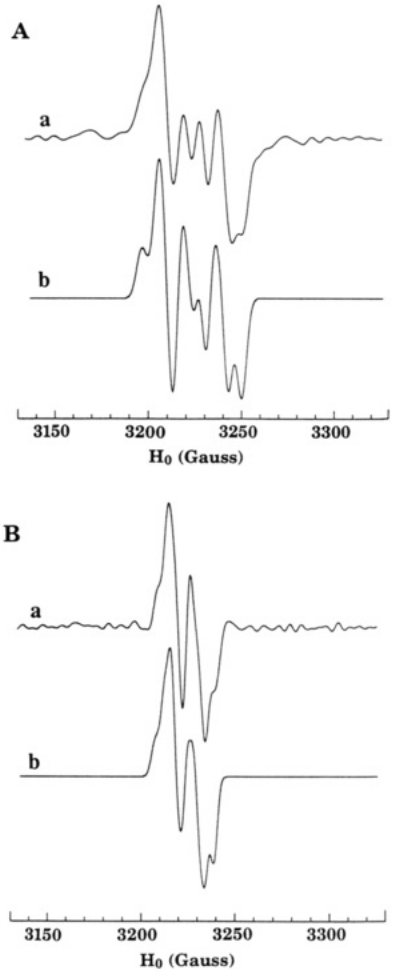

FIGURE 4: Comparison of resolution enhanced experimental (a) and computer simulated spectra (b) of samples prepared with L-[α-^{15}N]-lysine (A) and DL-[α-^{15}N, 2-^{2}H]lysine (B). The spectrum recorded experimentally for spectrum a in part A and spectrum a in part B are shown in spectra a and b of Figure 2, respectively. Resolution-enhanced spectra were obtained using (A, a) $\sigma = 6.5$ G and $L = 0.165$ G^{-1} and (B, a) $\sigma = 7.0$ G and $L = 0.220$ G^{-1}. Simulations were obtained using $g_{xx} = 2.0043$; $g_{yy} = 2.0037$, $g_{zz} = 2.0021$, $a^{15}_{N\beta} = 11.6$ G, for the β-^{1}H, $A_{xx} = A_{yy} = 3.6$ G, $A_{zz} = 8.8$ G, and Euler angles $\alpha = 3°$ and $\beta = -80°$; for α-^{1}H (A, b), $A_{xx} = 32.6$ G, $A_{yy} = 10.1$ G, $A_{zz} = 22.5$ G; for α-^{2}H (B, b), $A_{xx} = 5.0$ G, $A_{yy} = 1.6$ G, $A_{zz} = 3.5$ G. Line widths were (A, b) 3.2 G and (B, b) 2.4 G; 2025 crystal orientations were sampled in the simulations.

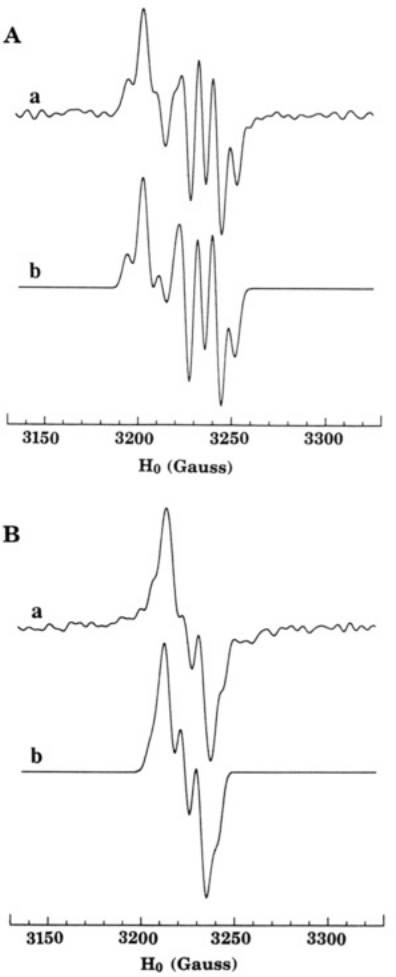

FIGURE 5: Comparison of resolution-enhanced experimental (a) and simulated spectra (b) of samples prepared with L-lysine (A) and DL-[2-^{2}H]lysine (B). The spectrum recorded experimentally for spectrum a in part A and spectrum a in part B are shown in spectra a and c of Figure 1, respectively. Resolution enhanced spectra were obtained using (A, a) $\sigma = 7.5$ G and $L = 0.190$ G^{-1} and (B, a) $\sigma = 6.0$ G and $L = 0.220$ G^{-1}. Simulations were obtained using $g_{xx} = 2.0043$, $g_{yy} = 2.0037$, $g_{zz} = 2.0021$, $\alpha^{14}_{N\beta} = 8.3$ G; for the β-^{1}H, $A_{xx} = A_{yy} = 3.6$ G, $A_{zz} = 8.8$ G, and Euler angles $\alpha = 3°$ and $\beta = -80°$; for α-^{1}H (A, b), $A_{xx} = 32.6$ G, $A_{yy} = 10.1$ G, $A_{zz} = 22.5$ G; for α-^{2}H (B, b), $A_{xx} = 5.0$ G, $A_{yy} = 1.6$ G, $A_{zz} = 3.5$ G. Line widths were (A,b) 2.8 G and (B,b) 2.9 G; 2025 crystal orientations were sampled in the simulations.

of the **g** tensor depends on the dihedral angle, χ (see below). From the small magnitude of isotropic β-proton splitting, it is apparent that the dihedral angle between the axis of the radical p orbital and the C3–H bond is near 70° (see below). The orientations of these two coordinate systems are, in turn, related by Euler angles, α and β (Rose, 1957). Assuming axial symmetry for this interaction, the principal values of the anisotropic component of the splitting are $2B$, $-B$, $-B$, where the value $2B$ holds along the z' axis of the principal axis of the hyperfine tensor. The Euler angles ($\alpha = 3°$, $\beta = -80°$) were calculated for $\chi = 70°$, and the best simulations were obtained with $B \sim 1.7$ G and $a_{\beta H} = 5.3 \pm 0.5$ G (Figure 5). The magnitude of B is comparable to that reported previously for β-protons (McConnell & Strathdee, 1959; Rowlands & Whiffen, 1961; Pooley & Whiffen, 1961; Fujimoto, et al., 1968). The hyperfine splittings obtained from the simulations are collected in Table I.

Calculation of the Dihedral Angles for β-Substituents. The isotropic hyperfine splittings arising from β-substituents in π-radicals are strongly dependent on the dihedral angle, χ,

Scheme III

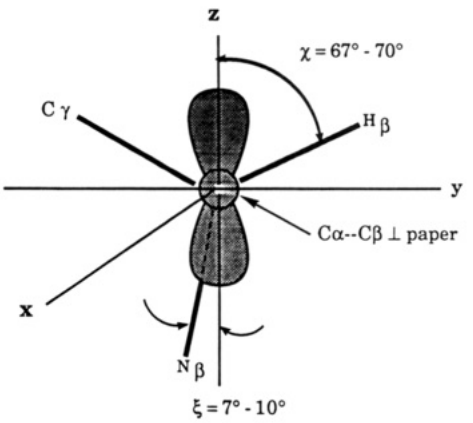

defined in Scheme III. For β-proton splittings, $a_{\beta H}$, the following relationship has been established:

$$a_{\beta H} = A_1 + A_2 \cos^2 \chi \qquad (3)$$

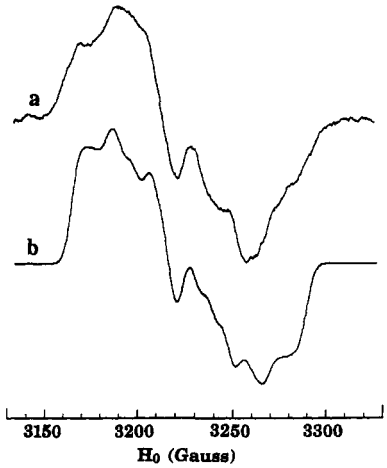

FIGURE 6: Comparison of experimental and simulated spectra of a sample with L-[2-^{13}C]lysine. The simulation was obtained using g_{xx} = 2.0043, g_{yy} = 2.0037, g_{zz} = 2.0021, α-^{13}C splitting, $A_{xx} = A_{yy}$ = 8.6 G, A_{zz} = 76 G, $a^{14}_{N\beta}$ = 8.3 G; for the β-^{1}H, $A_{xx} = A_{yy}$ = 3.6 G, A_{zz} = 8.8 G, and Euler angles α = 3° and β = –80°; for α-^{1}H, A_{xx} = 32.6 G, A_{yy} = 10.1 G, A_{zz} = 22.5 G. Line width = 4.6 G.

where A_1 and A_2 are empirically determined constants that have values of 0.92 G and 42.6 G, respectively, for unit spin density on C_α (Fischer, 1973). Adjusting the values of A_1 and A_2 for the 80% spin density at C2 (see below), and using $a_{\beta H}$ = 5.3 ± 0.5 G, χ is between 67° and 70°. In this conformation, the C3–N_β bond nearly eclipses one lobe of the $2p_z$ orbital at C2, i.e., $\xi \cong 7° - 10°$. This geometry is compatible with the large (8.3 ± 0.5 G) ^{14}N hyperfine splitting. The relatively large value of $a_{^{14}N}$ is consistent with the small value of ξ derived from the β-proton hyperfine splitting (Taniguchi et al., 1968). An isotropic hyperfine splitting of 550 G is expected for an unpaired electron in a 2s orbital on nitrogen (Wertz & Bolton, 1986). Thus, the spin density on the β-nitrogen is ~1.5%.

Spin Density on C2. The spin density on C2 in the radical may be estimated from the isotropic component of the α-proton hyperfine splitting. The relationship between the magnitude of the α-proton splitting constant, $a_{\alpha H}$, and α-carbon spin density, ρ, is described by the well-known McConnell relationship:

$$a_{\alpha H} \cong Q\rho \qquad (4)$$

where Q is an empirically determined constant with a value of ~27 G (Wertz & Bolton, 1986). In this case, $a_{\alpha H}$ = 21.7 G, and $\rho \cong 80\%$. The α-carbon spin density is similar to that reported for several other α-radicals of carboxylic acids (Morton, 1964).

2-^{13}C Hyperfine Splitting. The large, anisotropic hyperfine splitting from 2-^{13}C together with the multiplicity of hyperfine splittings (from the other three nuclei) spreads the spectral intensity and degrades S/N in the spectrum of the sample of [2-^{13}]lysine. Consequently this spectrum did not respond as well to resolution enhancement. A "first-order" simulation (see Figure 6) of this spectrum was computed using an α-^{13}C hyperfine tensor having values (see Table I) similar to those reported for the α-radical of malonic acid (Cole & Heller, 1961). The ratios of the anisotropic components of ^{13}C hyperfine tensor to the theoretical values provide an independent estimate (Wertz & Bolton, 1986) of spin density, ρ ~ 70%, at C2. This lower estimate of ρ places χ at the lower end of the range given in Scheme III. The estimated values of the ^{13}C hyperfine tensor in the present case, however, have greater uncertainty than that of $a_{\alpha H}$.

DISCUSSION

Simulations of the EPR spectra obtained in the steady state of the reaction of lysine 2,3-aminomutase for samples with lysine and its various isotopic forms account for all of the significant features in the spectra. The absence of "orphan signals" of appreciable amplitude indicates that the signals in the spectra come from a single, dominant organic radical. A structure for this steady-state radical emerges from the EPR results presented above (see Scheme III). This α-carbon radical of β-lysine corresponds to the product radical in the proposed mechanism for rearrangement (see Scheme I). Although the kinetic competency of this species as a catalytic intermediate and its attachment to PLP in the reaction have yet to be established, the position of the unpaired electron and the geometry of the radical are fully compatible with the notion that this species is indeed on the catalytic pathway.

The predominance of this product radical during the steady state of the reaction, and the absence of observable signals for any of its precursors, indicates that the α-carbon radical is more stable than the other three radicals shown in Scheme I. The possibility for delocalization of unpaired spin onto the adjacent carboxylate group of the α-radical likely accounts for the relative stability of this intermediate. The unpaired spin density on C2 is ~80%, and spin delocalization onto the carboxylate group likely accounts for much of the remainder of spin density in the radical. In the postulated azacyclopropylcarbinyl intermediate, delocalization of unpaired spin about the pyridinium ring of PLP would be expected to afford a stabilizing influence. However, the highly strained, three-membered ring in this species would presumably counteract this stabilization and give this radical a higher overall free energy. For example, in the ring opening of the cyclopropylcarbinyl-3-butenyl radical (i.e., an analogous rearrangement) the ring-opened form is favored by a factor of 10^4 (Effio et al., 1980).

The success of selective deuteration of the substrate in identification of the sources of hyperfine splitting in the EPR spectrum of the present enzyme-bound radical is in contrast to experiences with π-radicals that are generated by exposure of a host lattice to ionizing radiation. In the latter, deuteron or proton exchanges within the host lattice complicate the interpretations (Wertz & Bolton, 1986). The α-proton of the protein-based, glycyl radical of pyruvate formate-lyase is readily solvent-exchangeable (Wagner et al., 1992). Alkyl radicals are highly reactive, and the absence of such exchange reactions in the present case indicates that the radical centers in the intermediates are effectively isolated from other groups that might inadvertently participate in radical chain propagation reactions. In this regard, the EPR data clearly show that the radical is bound in a specific, rigid conformation. Any variations in the dihedral angle, χ, throughout the population of radicals in the sample would smear the hyperfine splitting from the β-substituents because of the $\cos^2 \chi$ dependence of β-proton (β-nitrogen) hyperfine splitting. The sharp definition of these splittings in the EPR spectra thus indicates that the rotational conformation about the C2–C3 bond is fixed throughout the population of radicals in the sample. The orientation of the C3-N_β bond (i.e., nearly eclipsed with the partially occupied p orbital) is fully compatible with the known stereochemistry of the reaction. During the mutation, the 3-*pro-R* hydrogen of lysine is transferred to the 2-*pro-R* position in the product, β-lysine (Aberhart et al., 1983), while the amino group is transferred intramolecularly from C2 to C3. The conformation of the radical is such that these transfers would occur along the top

and bottom (see Scheme III), respectively, of the lysine skeleton. In the reverse direction, the nitrogen is positioned to form a bond with C2 through combination of the unpaired electron with a π-electron from the presumed imino linkage.

Although solvent-exchangeable protons are not strongly coupled to the radical (Ballinger et al., 1992), the protonation state of the β-nitrogen in the radical cannot be determined unambiguously from the available data. Calculations based on the point–dipole approximation using distances from molecular models indicate that the magnitude of dipolar coupling between the unpaired electron and any protons on the β-nitrogen could escape detection in the CW EPR measurements. Furthermore, the lack of observable changes in the spectrum when [4,4,5,5-$^2H_4$]lysine is used as a substrate confirms that the splitting from protons attached to γ-positions (N_β and C4) are too small to detect in these spectra. The chemical precedent in the radical rearrangement of an aldimine (Han & Frey, 1990), however, provides support for the proposed linkage of lysine with PLP.

EPR spectroscopic evidence for radical intermediates has been obtained for B_{12}-dependent enzymes such as diol dehydrase (Finlay et al., 1973; Valinsky et al., 1974), glycerol dehydrase (Cockle et al., 1972), ribonucleotide reductase (Hamilton et al., 1972; Orme-Johnson et al., 1974), and ethanolamine ammonia lyase (Babior et al., 1974). For these enzymes, the EPR spectra contain signals from B_{12r} and from an organic radical. The signals of the organic radical exhibit features attributed to a magnetic coupling with the low-spin Co^{2+} in B_{12r} (Schepler et al., 1975; Pilbrow, 1982). For diol dehydrase (Valinsky et al., 1974) and ethanolamine ammonia lyase (Babior et al., 1974), the organic radical components in these spectra have been assigned to a free radical form of the substrate on the basis of observations of changes in the shapes of the signals coincident with isotopic substitutions in the substrate or substrate analogues. More recently, the origin of the organic radical component in the reaction of ethanolamine ammonia lyase has been reexamined (O'Brien et al., 1985). Pulsed EPR measurements provide evidence that the radical may be a protein-based radical which participates in an alternative pathway for hydrogen exchanges between the substrate radical and product (Tan et al., 1986).

Analysis of the EPR spectrum of the steady-state radical in the lysine 2,3-aminomutase reaction clearly shows that this radical is not strongly spin-coupled to other paramagnetic centers. The saturation properties of the EPR signals at 77 K, however, indicate that the radical may be in the vicinity of another paramagnetic center (Ballinger et al., 1992). Signals in the spectrum, however, narrow perceptively at 30 K (spectrum not shown), and this behavior suggests that the paramagnetic neighbor may be a reduced [Fe-S] cluster on the enzyme which may have thermally populated paramagnetic states at 77 K (R. M. Petrovich, F. J. Ruzicka, G. H. Reed, and P. A. Frey, unpublished observations). The aldimine derivatives of PLP and amino acids are known to chelate metal ions (Metzler & Snell, 1952). The relatively narrow EPR signals observed for the steady-state radical, however, show that any paramagnetic Co component of the enzyme is not chelated in this manner. Furthermore, if the initial generation of the 5′-deoxyadenosine-5′-yl results in production of a Co^{2+} species, magnetic interactions between this species and the radical are weak. Thus, the alternative metallocofactors and associated radical-initiation mechanism in lysine 2,3-aminomutase, together with the stability of the α-carbon radical, likely account for the extraordinarily clear view of the EPR spectrum of this substrate-based radical intermediate.

ACKNOWLEDGMENT

We are grateful to Drs. David Latwesen and Gary Wesenberg for their assistance with computer programming.

REFERENCES

Abeles, R. H., & Dolphin, D. (1976) *Acc. Chem. Res. 9*, 114–121.
Aberhart, D. J., Gould, S. J., Lin, H.-J. Thirubengadam, T. K., & Weiller, B. H. (1983) *J. Am. Chem. Soc. 105*, 5461–5470.
Armstrong, W. A., & Humphreys, W. G. (1967) *Can. J. Chem. 45*, 2589–2597.
Atherton, N. M., & Winscom, C. J. (1973) *Inorg. Chem. 12*, 383–390.
Babior, B. M., Moss, T. H., Orme-Johnson, W. H., & Beinert, H. (1974) *J. Biol. Chem. 249*, 4537–4544.
Ballinger, M. D., Reed, G. H., & Frey, P. A. (1992) *Biochemistry 31*, 949–953.
Baraniak, J., Moss, M. L., & Frey, P. A. (1989) *J. Biol. Chem. 264*, 1357–1360.
Battersby, A. R., Murphy, R., & Staunton, J. (1982) *J. Chem. Soc., Perkin Trans. 1* 449–453.
Brok, M., Babcock, G. T., De Groot, A., & Hoff, A. J. (1986) *J. Magn. Reson. 70*, 368–378.
Chirpich, T. P., Zappia, V., Costilow, R. N., & Barker, H. A. (1970) *J. Biol. Chem. 245*, 1778–1789.
Cockle, S. A., Hill, H. A. O., Williams, R. J. P., Davies, S. P., & Foster, M. A. (1972) *J. Am. Chem. Soc. 94*, 275–277.
Cole, T., & Heller, C. (1961) *J. Chem. Phys. 34*, 1085–1086.
Edmondson, D. E. (1978) *Biol. Magn. Reson. 1*, 205–237.
Effio, A., Griller, D., Ingold, K. U., Beckwith, A. L. J., & Serelis, A. K. (1980) *J. Am. Chem. Soc. 102*, 1734–1736.
Finlay, T. H., Valinsky, J., Mildvan, A. S. & Abeles, R. H. (1973) *J. Biol. Chem. 248*, 1285–1290.
Fischer, H. (1973) in *Free Radicals* (Kochi, J. K., Ed.) Vol. II, pp 435–491, Wiley, New York.
Frey, P. A. (1990) *Chem. Rev. 90*, 1343–1357.
Fujimoto, M., Seddon, W. A., & Smith, D. R. (1968) *J. Chem. Phys. 48*, 3345–3350.
Goodman, B. A., & Raynor, J. B. (1970) *Adv. Inorg. Chem. Radiochem. 13*, 135–362.
Hamilton, J. A., Tamao, Y., Blakeley, R. I., & Coffman, R. E. (1972) *Biochemistry 11*, 4696–4705.
Han, O., & Frey, P. A. (1990) *J. Am. Chem. Soc. 112*, 8982–8983.
Hecht, H. G. (1967) *Magnetic Resonance Spectroscopy*, p 129, Wiley, New York.
Hedberg, A., & Ehrenberg, A. (1968) *J. Chem. Phys. 48*, 4822–4828.
Horsefield, A., Morton, J. R., & Whiffen, D. H. (1961) *Mol. Phys. 4*, 425–431.
Kauppinen, J. K., Moffatt, D. J., Mantsch, H. H., & Cameron, D. G. (1981) *Appl. Spectrosc. 35*, 271–276.
Kilgore, J. L., & Aberhart, D. J. (1991) *J. Chem. Soc., Perkin Trans. 1*, 79–84.
Latwesen, D. G., Poe, M., Leigh, J. S., & Reed, G. H. (1992) *Biochemistry 31*, 4946–4950.
McConnell, H. M., & Strathdee, J. (1959) *Mol. Phys. 2*, 129–138.
McConnell, H. M., Heller, C., Cole, T., & Fessenden, R. W., (1960) *J. Am. Chem. Soc. 82*, 766–775.
Metzler, D. E., & Snell, E. E. (1952) *J. Am. Chem. Soc. 74*, 979–983.
Morton, J. R. (1964) *Chem. Rev. 64*, 453–471.
Moss, M. L., & Frey, P. A. (1987) *J. Biol. Chem. 262*, 14859–14861.
Moss, M. L., & Frey, P. A. (1990) *J. Biol. Chem. 265*, 18112–18115.
O'Brien, R. J., Fox, J. A., Kopezynski, M. G., & Babior, B. M. (1985) *J. Biol. Chem. 260*, 16131–16136.

Orme-Johnson, W. H., Beinert, H., & Blakley, R. L. (1974) *J. Biol. Chem. 249*, 2338–2343.
Paul, H., & Fischer, H. (1969) *Ber. Bunsen-Ges. Phys. Chem. 73*, 972–980.
Petrovich, R. M., Ruzicka, F. J., Reed, G. H., & Frey, P. A. (1991) *J. Biol. Chem. 266*, 7656–7660.
Pilbrow, J. R. (1982) in B_{12} (Dolphin, D., Ed.) Vol. 1, pp 431–462, Wiley-Interscience, New York.
Pooley, D., & Whiffen, D. H. (1961) *Mol. Phys. 4*, 81–86.
Rieger, P. H. (1982) *J. Magn. Reson. 50*, 485–489.
Rose, M. E. (1957) *Elementary Theory of Angular Momentum*, pp 50–51, Wiley, New York.
Rowlands, J. R., & Whiffen, D. H. (1961) *Mol. Phys. 4*, 349–351.
Stubbe, J. A. (1989) *Annu. Rev. Biochem. 58*, 257–285.
Schepler, K. I., Dunham, W. R., Sands, R. H., Fee, J. A., & Abeles, R. H. (1975) *Biochim. Biophys. Acta 397*, 510–518.
Tan, S. L., Kopezynski, M. G., Bachovchin, W. W., Orme-Johnson, W. H., & Babior, B. M. (1986) *J. Biol. Chem. 261*, 3483–3485.
Taniguchi, H., Fukui, K., Ohnishi, S., Hatano, H., Hasegawa, H., & Maruyama, T. (1968) *J. Phys. Chem. 72*, 1926–1931.
Valinsky, J. E., Abeles, R. H., & Mildvan, A. S. (1974) *J. Biol. Chem. 249*, 2751–2755.
Wagner, A. F. V., Frey, M., Neugebauer, F. A., Schafer, W., & Knappe, J. (1992) *Proc. Natl. Acad. Sci. U.S.A. 89*, 996–1000.
Wertz, J. E., & Bolton, J. R. (1986) *Electron Spin Resonance*, pp 164–174, Chapman and Hall, New York.